Acta Cryst. (1963). **16**, 129

Determination of Bond Angles in δ-BHC Crystal by the Zeeman Effect of Nuclear Quadrupole Resonance Spectrum

By Yonezo Morino, Masaharu Toyama and Koichi Itoh*

Department of Chemistry, Faculty of Science, The University of Tokyo, Bunkyo-ku, Tokyo, Japan

(*Received* 23 *January* 1962)

The Zeeman effect of the chlorine nuclear quadrupole resonance of δ-benzene hexachloride was observed. The six absorption lines were assigned to the six chlorine atoms in the molecule, referring to the result of the X-ray diffraction by A. J. van Bommel *et al.* The locations of the principal *z* axes of the field gradients were determined with the uncertainty from 0·1° to 0·5°, and the C–Cl bonds were found to be considerably distorted from the tetrahedral angle. The asymmetry parameters of the electric field gradients were found to be 0·00 ± 0·01, 0·034 ± 0·007, 0·020 ± 0·005, 0·037 ± 0·010, 0·023 ± 0·008, and 0·015 ± 0·010, respectively, for the six chlorine atoms corresponding to the resonance lines in the order of decreasing frequency. The asymmetry of the field gradient is most likely to be due to the crystalline field rather than to the double-bond character which is the main origin of the asymmetry for aromatic compounds.

Introduction

Zeeman effect of the nuclear quadrupole resonance spectrum in a single crystal is useful for locating the principal axes of the electric field gradient at the nucleus arising from the surrounding charges. If the directions of the principal axes of the field gradient with respect to individual molecules are known, relative orientation of the molecules in the crystal is determined by a Zeeman study. For the chlorine nucleus in a C–Cl bond, it can safely be assumed that the principal *z* axis, the direction of the maximum principal value of the field gradient, is along the C–Cl bond. For instance, Dean *et al.* (1958) confirmed the coincidence of the direction of the maximum principal axis with the bond direction for 1,2,4,5-tetrachlorobenzene, by the simultaneous measurements of the Zeeman effect and the X-ray diffraction. Kikuchi, Hirota & Morino (1961) obtained another evidence for this assumption in the case of gaseous propargyl bromide by analysing the quadrupole hyperfine structure of the microwave absorption spectrum.

On the other hand, when the crystalline structure is known by some other means, the Zeeman study enables us to assign each of the observed resonance lines to different nucleus in the crystal. Thus the six distinct lines of the Cl^{35} pure quadrupole resonance of the α-isomer of BHC were assigned to the six chlorine atoms in a molecule by the Zeeman effect, based on the crystal structure obtained from the X-ray diffraction. Similar assignment was done also for the γ-isomer (Morino *et al.*, 1959). A purpose of the present study is to determine the directions of the principal axes of the field gradients in the crystal lattice of δ-BHC and to make the assignment of the six absorption lines.

The δ-BHC molecule has five equatorial C–Cl bonds and a single axial C–Cl bond, one for each carbon atom. The crystal structure has been determined by van Bommel *et al.* (1950) with the X-ray diffraction. Their result shows that the crystal is monoclinic, belonging to the space group $P2_1/c$ with the lattice constants:

$$a = 9{\cdot}64,\ b = 8{\cdot}73,\ c = 14{\cdot}09\ \text{Å},\ \beta = 118°,\ Z = 4\ .$$

Four molecules in a unit cell are all equivalent, but six chlorine atoms in each molecule occupy the lattice sites non-equivalent to one another. The four equivalent C–Cl bonds of all the molecules in the unit cell are arranged either antiparallel to each other or symmetric with respect to the *ac* plane. In other words, for each of the six absorption lines there are two distinct field gradient tensors symmetric with respect to the *ac* plane for each set of equivalent chlorine atoms.

Another important information to be obtained by the Zeeman study is the asymmetry parameter of the electric field gradient. The field gradient has been found to be asymmetric in aromatic or heterocyclic compounds which have some double-bond nature by resonances. This article will report the result of the measurement of the asymmetry parameters of the chlorine atoms in δ-BHC which has only aliphatic σ-bonds.

Experimental and results

The spectrometer used was of a conventional type with a self-quenched super-regenerative oscillator-detector, the quench frequency being about 50 kcyc./sec. A narrow band amplifier and a phase sensitive detector were used with a pen-recorder in order to attain the sensitivity high enough for the detection of such a weak spectrum as that of δ-BHC. The magnetic field for the Zeeman study was furnished

---

* Present address: The Institute for Solid State Physics, The University of Tokyo, Minato-ku, Tokyo, Japan.

by an air-cooled Helmholtz coil (Morino *et al.*, 1958), and adjusted for an absorption line at a suitable strength between 50 and 150 gauss, not to be disturbed by the neighbouring absorption lines. The orientation of the magnetic field covered 360° for the azimuthal traverse, but only about 35° for the polar traverse because the vertical lead-wire of the r.f. tank-coil hindered the Helmholtz coil to turn further. Both the azimuthal and polar angles were read by means of a scale on the goniometer to within 0·1°.

The δ-BHC was recrystallized from benzene solution. Single crystals were prepared from the saturated benzene solution by evaporating the solvent carefully. The r.f. coil was wound directly around the single crystal which is approximately 10 mm. in diameter and 50 mm. in length. The direction of the crystal c axis was almost parallel to the axis of the r.f. coil.

The six pure quadrupole resonance frequencies of δ-BHC are 37·268, 36·818, 36·364, 36·256, 36·228, and 35·948 Mc/sec. at room temperature (Morino *et al.*, 1956). For convenience they are designated as A to F in the order of decreasing frequency. Since the frequencies C, D, and E are close to each other and their separations are of the same order as either of the Zeeman splitting or of the quench frequency, their Zeeman patterns show very complicated features.

The method of 'no- or zero-splitting locus' (Das & Hahn, 1958) was employed for determining the location of the principal z axis (hereafter x, y, and z denote the principal axes of the field gradient tensor). The curvature of an elliptical cone of the no-splitting locus can be used to locate the principal x and y axes and to obtain the asymmetry parameter η. However, for the precise measurement of η, the method is not suitable for our apparatus in which the magnetic field covers only a restricted region of the direction in space, and especially when the asymmetry parameter is small. Therefore the asymmetry parameter was determined from the splitting by the static magnetic field applied parallel to the principal xy plane. The locations of the principal x and y axes were determined by measuring the dependence of the relative intensity of the Zeeman components upon the direction of the r.f. field.

When a static magnetic field is applied nearly parallel to the principal xy plane of the field gradient whose asymmetry parameter is small, the relative intensity P_r is given for the spin $I=3/2$ to the first order in η as follows (Toyama, 1959):

$$P_r = P(-)/(P(+)+P(-)) = \tfrac{1}{2}[1-(\eta/\Delta\nu)\cos 2\varphi_r]\,, \quad (1)$$

and

$$\Delta\nu = (\eta^2 + 9\cos^2\theta)^{\frac{1}{2}}, \quad (2)$$

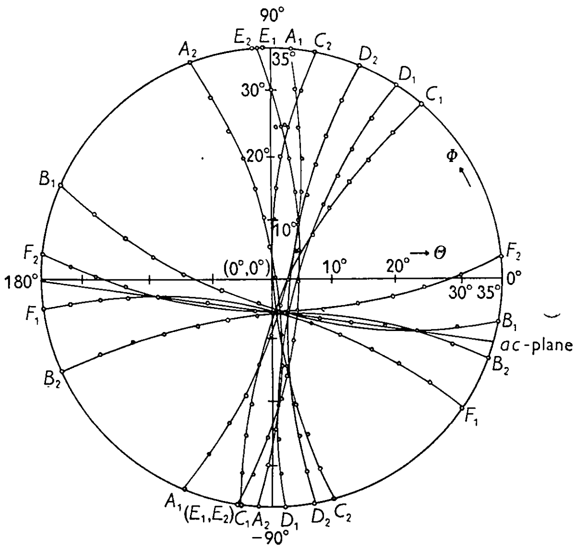

Fig. 1. Stereogram of the observed no-splitting loci. For all the absorption lines, the loci corresponding to the two field gradient tensors symmetric with respect to the ac plane to each other join in the vicinity of the pole, which is nearly parallel to the crystal c axis.

where $P(+)$ and $P(-)$ denote the intensities of the inner and the outer pairs of the Zeeman components, respectively, and $\Delta\nu$ one-half of the frequency difference of the separations of the two pairs. (θ_r, φ_r) and (θ, φ) are the direction of the r.f. field and that of the static magnetic field with respect to the principal axes, respectively.

In order to find out the no-splitting loci, the spectrum was recorded for various orientations of the static field at 1° intervals along the circle which traversed the loci perpendicularly. The peak-to-peak separation of the first derivatives was measured for the no-splitting Zeeman components of the absorption line and plotted against the orientation. The no-splitting locus was obtained from the orientations giving the minimum separation which should be equal to the line width of a single Zeeman component. The uncertainty introduced in this process was about 0·2°. Fig. 1 shows the no-splitting loci in a stereographic projection, where the polar coordinates (Θ, Φ) denote the laboratory coordinate system. In this stereogram Θ and Φ are projected on a horizontal plane through the origin fixed at the sample, so that the directions in a great circle on the sphere are projected into a straight line. Since each absorption line comes from two field gradient tensors with different orientations, as mentioned above, twelve no-splitting loci were observed. Here, A_1 and A_2 denote the field gradient tensors belonging to the absorption line A due to the molecules 1 and 2, respectively, which are mutually symmetrical with respect to the ac plane. They can be determined uniquely from the condition that the observed principal z axes of the individual C–Cl bonds in a molecule are nearly parallel or make an angle close to the tetrahedral angle.

The principal axes and the asymmetry parameters were determined by the following procedure. The locations of the principal z axes were first roughly determined from the observed no-splitting loci on the assumption of $\eta = 0$. Next the crystal *b* axis and hence the *ac* plane were precisely determined by referring to the symmetry with respect to the *ac* plane. Then the *x* and *y* axes and the asymmetry parameter were determined in the *ac* plane. Finally the locations of the *z* axes were refined by taking into account the asymmetry of the field gradient thus obtained, through an application of the method of least-squares.

Table 1. *The direction cosines of the principal z axes for the molecule* 1 *and* 2, *with reference to the crystal-fixed coordinate system*

	X	Y	Z	σ
A_1	$0{\cdot}5633 \pm 0{\cdot}0011$	$-0{\cdot}8114 \pm 0{\cdot}0013$	$0{\cdot}1561 \pm 0{\cdot}0022$	8′
A_2	$0{\cdot}5640 \pm 0{\cdot}0009$	$-0{\cdot}8111 \pm 0{\cdot}0003$	$-0{\cdot}1550 \pm 0{\cdot}0022$	6′
B_1	$0{\cdot}5713 \pm 0{\cdot}0021$	$0{\cdot}1219 \pm 0{\cdot}0025$	$0{\cdot}8116 \pm 0{\cdot}0018$	10′
B_2	$0{\cdot}5708 \pm 0{\cdot}0026$	$0{\cdot}1213 \pm 0{\cdot}0049$	$-0{\cdot}8120 \pm 0{\cdot}0011$	15′
C_1	$0{\cdot}6066 \pm 0{\cdot}0025$	$0{\cdot}7709 \pm 0{\cdot}0026$	$-0{\cdot}1944 \pm 0{\cdot}0029$	13′
C_2	$0{\cdot}6072 \pm 0{\cdot}0024$	$0{\cdot}7712 \pm 0{\cdot}0013$	$0{\cdot}1912 \pm 0{\cdot}0034$	12′
D_1^{I}	$0{\cdot}5760 \pm 0{\cdot}0017$	$0{\cdot}8134 \pm 0{\cdot}0013$	$-0{\cdot}0818 \pm 0{\cdot}0021$	8′
D_2^{I}	$0{\cdot}5760 \pm 0{\cdot}0028$	$0{\cdot}8138 \pm 0{\cdot}0016$	$0{\cdot}0773 \pm 0{\cdot}0038$	13′
D_1^{II}	$0{\cdot}5755 \pm 0{\cdot}0017$	$0{\cdot}8158 \pm 0{\cdot}0013$	$-0{\cdot}0576 \pm 0{\cdot}0021$	8′
D_2^{II}	$0{\cdot}5762 \pm 0{\cdot}0028$	$0{\cdot}8155 \pm 0{\cdot}0016$	$0{\cdot}0537 \pm 0{\cdot}0038$	13′
E_1	$0{\cdot}6044 \pm 0{\cdot}0062$	$-0{\cdot}7962 \pm 0{\cdot}0049$	$0{\cdot}0279 \pm 0{\cdot}0076$	30′
E_2	$0{\cdot}6044 \pm 0{\cdot}0062$	$-0{\cdot}7962 \pm 0{\cdot}0049$	$-0{\cdot}0279 \pm 0{\cdot}0076$	30′
F_1	$0{\cdot}5694 \pm 0{\cdot}0018$	$-0{\cdot}1234 \pm 0{\cdot}0032$	$-0{\cdot}8127 \pm 0{\cdot}0016$	11′
F_2	$0{\cdot}5706 \pm 0{\cdot}0023$	$-0{\cdot}1194 \pm 0{\cdot}0049$	$0{\cdot}8125 \pm 0{\cdot}0011$	12′

The final values of the angles of the directions of the principal *z* axes are tabulated in Table 1, where *X*, *Y*, and *Z* denote the crystal-fixed coordinate system in which the *Z* axis is taken parallel to the crystal *b* axis so that the *XY* plane coincides with the *ac* plane. As neither the *a* nor the *c* axis can be determined from the Zeeman study, the *X* axis is taken along the direction bisecting the projections of *B* and *F* in the *XY* plane, because the bisecting line was found to be nearly along the *c* axis as will be described later. The last column in Table 1 denotes σ, the standard deviation of the direction of the principal *z* axis thus obtained. Owing to the symmetry with respect to the *ac* plane, A_1 and A_2 should have the same direction cosines except for the sign of *Z*. The discrepancies indicate the errors of this analysis, though they are certainly within the standard deviation. As shown in Fig. 1, E_1 and E_2 were not resolved except for the points near the rim, because they are almost parallel to the *ac* plane. Accordingly, the uncertainties of E_1 and E_2 are larger than the others. Two orientations for the line *D* arise from two possible orientations of the *x* and *y* axes which will be discussed later.

The asymmetry parameters were measured by scanning of the magnetic field in the *XY* plane, *i.e.*, in the *ac* plane. The two tensors associated with one absorption line are equivalent when the external magnetic field lies in this plane of symmetry, so that the overall Zeeman pattern reduces to a simple one, *i.e.*, in general, to a four-line pattern. Another symmetry plane exists, for each set of field gradient tensors, perpendicularly to the *ac* plane. The intersection of the *xy* plane with the *ac* plane was easily found, because it coincides with that of these two symmetry planes. Fig. 2 shows a typical pattern of the splittings and the relative intensities. In each chart the spectrum was recorded from the right to left with a static magnetic field parallel to, and 0·75° and 1·75° apart from the intersection of the *xy* and *ac* planes. The intensities of the outer components are smaller than those of the inner ones for the line *B*, whereas they are larger for the line *C*. Although the line *B* shows a distinct doublet in the principal *xy* plane, the line *C* shows a broad and apparently single line in the *xy* plane. It arises from the fact that the intensities of the inner components of the line *C* rapidly decrease as the magnetic field comes close to the *xy* plane.

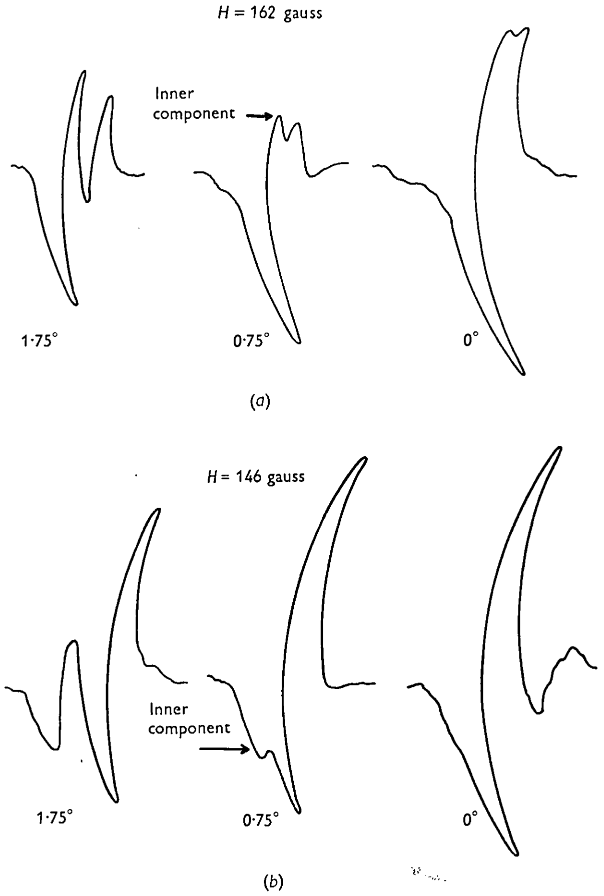

Fig. 2. Typical pattern of the Zeeman splittings. The Zeeman components on the higher frequency side were recorded in the first derivative forms. The frequency increases from left to right. (*a*) Absorption line *B*; (*b*) absorption line *C*.

When two absorption lines come closer to within their own line width, the apparent peak-to-peak separation of the first derivative becomes smaller than the true one. In such cases the splittings and the relative intensities were obtained by calculating the first derivative of the composite of two Gaussian curves having a given separation and given relative intensity and by comparing it with the observed spectra. The observed asymmetry parameters and the locations of the r.f. field with respect to the principal axes are given in Table 2. For the line *A* asymmetry was not detected within the accuracy of the experiment. In this observation the r.f. field was assumed to be parallel to the axis of the r.f. coil, i.e., the *X* axis. The uncertainty of this assumption was estimated to be about 10°. The sign of φ_r could not be determined uniquely because either of the signs gives the same value of $\cos 2\varphi_r$ (see equation (1)). In principle, it is possible from the measurement of the relative intensity to make choice between φ_r and $-\varphi_r$. The theoretical calculation has shown that the dependence of the relative intensity upon the direction of the static magnetic field should be asymmetric with respect to the planes *xy*, *yz* and *zx*, because it depends upon the asymmetry parameter and the cross terms of the r.f. field $H_{rx}H_{ry}$, $H_{ry}H_{rz}$, and $H_{rz}H_{rx}$ (Toyama, 1959). In the present study, however, the stability of the oscillation frequency did not allow to detect such a slightly asymmetric change in the intensity.

Table 2. *The asymmetry parameters and the locations of the r.f. magnetic field, with reference to the principal axes (molecule* 1)

Absorption line	η	θ_r	$\lvert\varphi_r\rvert$
A	0·00 ± 0·01	—	—
B	0·034 ± 0·007	55° ± 10°	34° ± 15°
C	0·020 ± 0·005	53° ± 10°	90° ± 40°
D	0·037 ± 0·010	55° ± 10°	60° ± 20°
E	0·023 ± 0·008	53° ± 10°	20° ± 30°
F	0·015 ± 0·010	55° ± 10°	20° ± 25°

Table 3. *The direction cosines of the principal x and y axes, with reference to the crystal-fixed XYZ coordinate system (molecule* 1)

		X	*Y*	*Z*
B	*x*	0·67	−0·63	−0·39
	y	0·47	0·77	−0·43
C	*x*	0·00	0·24	0·97
	y	0·80	−0·59	0·14
D^{I}	*x*	0·41	−0·21	0·89
	y	0·71	−0·53	−0·46
D^{II}	*x*	0·41	−0·36	−0·84
	y	−0·71	0·45	−0·54
E^{I}	*x*	0·75	0·58	0·32
	y	0·27	0·17	−0·95
E^{II}	*x*	0·75	0·56	−0·36
	y	−0·27	−0·24	−0·93
F^{I}	*x*	0·77	0·42	0·48
	y	0·28	−0·90	0·33
F^{II}	*x*	0·77	−0·26	0·58
	y	−0·28	−0·96	−0·05

From the results given in Table 2 the locations of the principal *x* and *y* axes with reference to the crystal-fixed *XYZ* coordinate system were calculated and are given in Table 3. Two orientations for each of the absorption lines *D*, *E*, and *F* are obtained because of the ambiguity of the sign of φ_r which was described above. Alternative choices of the *x* and *y* axes give an influence on the location of the principal *z* axis as shown in Table 1. Fortunately, the choice makes little difference except for the line *D* according to the following reasons: for the lines *E* and *F* the asymmetry is so small that in either case the principal *z* axis agrees within about 10′ with the one calculated by assuming axial symmetry; for the line *C* the *x* and *y* axes are determined uniquely, though with considerable errors, since φ_r is nearly 90°. The determination of the asymmetry for the line *B* will be described in the following.

Table 4. *The observed and the calculated angles between the intersection of the xy plane of each q-tensor with the XY plane*

	Observed	Calculated	Difference
∠ *AE*	2° 40′	2° 24′	16′
∠ *AF*	42° 59′	43° 11′	12′
∠ *EF*	40° 22′	40° 47′	25′
∠ *BC*	39° 06′	39° 47′	41′
∠ BD^{I}	42° 02′	42° 41′	39′
∠ BD^{II}	42° 02′	42° 45′	43′
∠ CD^{I}	2° 52′	2° 54′	2′
∠ CD^{II}	2° 52′	2° 58′	6′

Table 4 shows the observed mutual angles made by the intersections of the *xy* plane of each field gradient tensor with the *XY* plane. They were obtained in the process of measuring the asymmetry parameters. The calculated values were obtained from the locations of the principal *z* axes given in Table 1. The notation ∠*AE*, for example, denotes the angle between the intersection of *A* and that of *E*. The angles between the two groups (*A*, *E*, *F*) and (*B*, *C*, *D*) could not be measured accurately, since the scanning of the static magnetic field was limited as described above. The satisfactory agreement is a good measure for the accuracy of the present crystal analysis. The ambiguity in the sign of φ_r for the line *B* was excluded by the consideration of this agreement. The excluded choice for the *x* axis gave the difference of about 3° either in ∠*BC* or in ∠*BD* between the observed and the calculated values. The difference exceeds the present experimental uncertainty which is shown in Table 1. On the other hand, ∠*BD* and ∠*CD* are not influenced, as shown in Table 4, whichever choice for *D* may be taken. Accordingly the alternative choice shown in Table 1 cannot be excluded for *D*. The deviation of the *z* axis from the value calculated on the assumption of the axial symmetry is 40′ in this case.

Table 5. *Atomic parameters of δ-BHC obtained by X-ray diffraction (van Bommel)*

The accuracy is about ±0·005 for chlorine atoms, and somewhat larger for carbon atoms. The C_3–Cl_3 bond corresponds to the axial one

	a	*b*	*c*
Cl_1	0·430	0·147	0·242
Cl_2	0·394	0·272	0·447
Cl_3	0·730	0·136	0·622
Cl_4	0·019	0·364	0·658
Cl_5	0·055	0·228	0·458
Cl_6	0·772	0·014	0·303
C_1	0·592	0·156	0·378
C_2	0·575	0·306	0·436
C_3	0·708	0·311	0·553
C_4	0·856	0·333	0·530
C_5	0·883	0·189	0·475
C_6	0·739	0·180	0·358

Finally the six absorption lines were assigned to the chlorine atoms in the crystal, by referring to the results of X-ray diffraction given in Table 5. In this process there occurred eight possible combinations, since the uncertainty of the data of the X-ray diffraction is too large to distinguish the small differences detected by the present Zeeman study; the uncertainty of the X-ray analysis is about ±4° for the direction of the C–Cl bond, roughly ten times as large as that of the present study. The assignment was made by referring to a reliability factor defined by

$$\langle \varDelta\theta^2 \rangle^{\frac{1}{2}} = \{\tfrac{1}{6} \sum_{i=1}^{6} (\varDelta\theta_i)^2\}^{\frac{1}{2}}\,, \tag{3}$$

where $\varDelta\theta_i$ denotes the angle between the direction of the *i*th C–Cl bond obtained by the X-ray diffraction and that of the principal *z* axis of the corresponding chlorine atom. Here it is required to describe these two systems in the same coordinate system. The *X* axis was taken as described before, because the absorption lines *B* and *F* are to be assigned to either of the bonds 3 and 6 (Table 6), and because the direction bisecting the projections of these two bonds in the *ac* plane is along the *c* axis. There is no assurance, however, that the *X* axis coincides exactly with the crystal *c* axis. This difficulty was avoided by taking the coordinate system which provides the least values of the reliability factor mentioned above with the aid of the least-squares method for each of the eight cases. The result is given in Table 6, which indicates that the assignment IV is the most probable one.

Table 6. *The reliability factor and the assignment of absorption lines to* C–Cl *bonds*

The number denotes a bond after Table 5.
The bond 3*a* corresponds to the axial one

	A	*B*	*C*	*D*	*E*	*F*	$\langle \varDelta\theta^2 \rangle^{\frac{1}{2}}$
I	1	6	2	5	4	3*a*	5° 54′
II	4	6	2	5	1	3*a*	4° 10′
III	1	6	5	2	4	3*a*	5° 22′
IV	4	6	5	2	1	3*a*	3° 19′
V	2	3*a*	1	4	5	6	6° 04′
VI	5	3*a*	1	4	2	6	5° 54′
VII	2	3*a*	4	1	5	6	4° 56′
VIII	5	3*a*	4	1	2	6	4° 45′

Discussion

First of all, it must be mentioned that the locations of the *z* axes of the field gradient tensors were determined with a good accuracy. The result is supported by the agreement of the absolute values of direction cosines of the molecule 1 with those of the molecule 2, as shown in Table 1, in conformity with the symmetry requirement. The question, to what extent the principal *z* axis of the field gradient tensor is parallel to the bond direction in the crystal, would be answered more accurately when the X-ray analysis is made with an accuracy comparable with that of the present study. Furthermore, the assignment of the absorption lines would be made more definite by the refined X-ray measurement. In this sense the refinement of the X-ray analysis of the crystal structure would be of much interest for δ-BHC.

Table 7. *The mutual angles between the principal z axes in the molecule*

F was assigned to the axial bond. The tetrahedral angle is 109° 28′, its supplement being 70° 32′

	B(6)	*C*(5)	*D*(2)	*E*(1)	*F*(3)
A(4)	110° 28′	71° 41′	110° 20′	172° 14′	72° 54′
B(6)		73° 35′	111° 49′$(^1)$	74° 16′	110° 25′
C(5)			172° 13′$(^2)$	104° 38′	114° 06′
D(2)				72° 23′	73° 30′$(^3)$
E(1)					114° 49′

$(^1)$ 111° 13′, 112° 26′.
$(^2)$ 172° 56′, 171° 35′.
$(^3)$ 72° 54′, 74° 06′.

The mutual angles of the principal *z* axes were calculated from the results listed in Table 1 and are given in Table 7 with the assigned C–Cl bonds in parentheses. For the sake of simplicity, averaged values are listed for the line *D*. To be more exact, the angles marked $(^1)$, $(^2)$, and $(^3)$ should be replaced by the three pairs of values shown beneath the table, corresponding to D^{I} and D^{II}. The other two angles related to *D* are not influenced whichever choice may be taken, the difference being within 3′. It should be noticed that the opposite equatorial bonds *A* and *E*, and *C* and *D* are not parallel: the deviations amount to 7° 46′ and 7° 47′ (precisely speaking, 7° 04′ or 8° 25′ for the latter pair), respectively. The other bond pair, *B* and *F*, is to make an angle close to the tetrahedral angle, because one of the bonds is an axial one, whereas the other is an equatorial one. It is seen from Table 7 that there exist considerable distortions. The distortions may be mainly due to the intermolecular forces. If the distortions were caused by intramolecular forces, they should be symmetric with respect to the plane of symmetry which the free molecule has. However, the actual form found in the crystal deviates appreciably from this symmetry.

The asymmetry parameters observed are comparable with those of the iodine atoms in iodoalkanes (Kojima *et al.*, 1953; Robinson *et al.*, 1954), but larger than expected from the molecular structure. They amount nearly to a half of the value of the asymmetry parameter in *p*-dichlorobenzene, (Morino & Toyama, 1961) and to one third of those in 1,3,5-trichlorobenzene (Morino & Toyama, 1960) and in 1,2,4,5-tetrachlorobenzene (Dean *et al.*, 1958). The asymmetry of the field gradient at the chlorine nucleus in a C–Cl bond has usually been interpreted by the partial double-bond character of the C–Cl bond formed by the lone-pair electrons on the chlorine atom. This is the case in the aromatic or vinyl compounds where the carbon atom attached to the chlorine atom has sp^2 hybrid orbitals and the electrons on the remaining $3p$ orbit perpendicular to the sp^2 plane participate in the conjugation. In the case of δ-BHC, however, the carbon atom has an sp^3 hybrid structure. It follows that the conjugation may not be present, or, if any, it will take place symmetrically with respect to the C–Cl bond.

Two effects should be mentioned in relation to the interpretation of the observed asymmetry. One is the deviation of the hybridization of the carbon atoms from the pure sp^3, as anticipated from the distortion of the bond angles observed above. When the skeleton of the molecule is deformed from the sp^3 configuration, the double-bond character of the C–Cl bond would increase. Unfortunately, the accuracy of the molecular structure determined by the X-ray diffraction is not sufficient to correlate the asymmetry with the distortion of the bond angles. It is likely, however, that the double-bond character does not take as important part in the asymmetry in this molecule. If the asymmetry arises from the double-bond character alone, the direction of the x axis should be related more or less to the symmetry of the molecule. The observed direction of the x axis of the bond 6*e*, to which the line *B* is assigned, shows no correlation with the symmetry of the molecule as shown in Fig. 3, though the uncertainty of the angle determination is ±15° (Table 2). It is quite the same even if the line *B* is assigned to the bond 3*a* (Table 7).

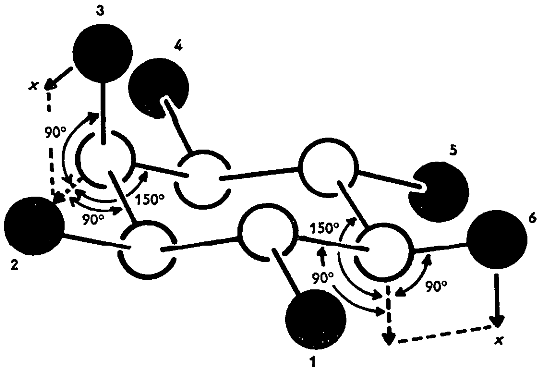

Fig. 3. The location of the principal x axis of *B*, which is shown in the solid arrow parallel to the dotted one.

Another effect to be considered is the one due to the electric charges on the neighboring atoms. As is easily seen, the direct field gradient due to the neighboring atoms is too small to produce the observed asymmetry. However, the direct field gradient distorts the electronic cloud around the chlorine nucleus to produce an indirect field gradient with a considerable strength. Sternheimer (1954) has theoretically shown that the total field gradient due to the neighboring atoms may be approximated by the direct one times a constant factor. In fact, the splittings of the six absorption lines in α- and γ-BHC with the total spread of about 1 Mc have been satisfactorily interpreted in terms of this effect by assuming a multiplying factor ~ 50 (Morino *et al.*, 1959). The asymmetry of $\eta = 0{\cdot}03$ is equivalent to the difference of about 1 m.c. between the coupling constant eQq_{xx} and eQq_{yy}. This is of the same order of magnitude as the total spreading of the six absorption lines so that it may be interpreted in a similar way. Thus it is most likely that the observed asymmetry is mainly due to the field gradient originated from the charge distribution in the crystal. This conclusion does not conflict with the results obtained up to the present, that the asymmetry comes predominantly from the double-bond character for aromatic C–Cl bonds.

For iodine nuclei in *saturated* compounds the asymmetry parameters have been obtained by the measurement of the two resonance lines. However, for Cl^{35} nucleus, whose spin is 3/2, the Zeeman study is the only method to obtain the asymmetry parameter. In this sense it is to be emphasized that the present study is the first case where the asymmetry parameter of a chlorine atom substituted to the *saturated* hydrocarbons has been observed by the Zeeman effect.

The authors express their sincere thanks to Dr Hideo Sueta, Research Laboratory of Mitsubishi Chemical Industry, Ltd and Dr Toshio Fujita, College of Agriculture, Kyoto University, for their kind supply of the pure sample of δ-BHC. They are also indebted to Dr Takashi Shimozawa, Department of Chemistry, St. Paul University, for the preparation of the single crystals used in this research. The expenses of the work were defrayed from the Ministry of Education of Japan to which their thanks are also due.

References

Das, T. P. & Hahn, E. L. (1958). *Nuclear Quadrupole Resonance Spectroscopy*. New York: Academic Press.

Dean, C., Pollak, M., Craven, B. M. & Jeffrey, G. A. (1958). *Acta Cryst.* **11**, 710.

Kikuchi, Y., Hirota, E. & Morino, Y. (1961). *Bull. Chem. Soc. Japan*, **34**, 348.

Kojima, S., Tsukada, K., Ogawa, S. & Shimauchi, A. (1953). *J. Chem. Phys.* **21**, 2237.

Morino, Y., Miyagawa, I., Chiba, T. & Shimozawa, T. (1956). *J. Chem. Phys.* **25**, 185.

Morino, Y., Chiba, T., Shimozawa, T. & Toyama, M. (1958). *J. Phys. Soc. Japan*, **13**, 869.

Morino, Y., Chiba, T., Shimozawa, T., Toyama, M. & Ito, K. (1959). *Rev. Univ. des Mines*, 9e Ser. T. XV, 591.

Morino, Y. & Toyama, M. (1960). *J. Phys. Soc. Japan*, **15**, 288.

Morino Y. & Toyama, M. (1962). *J. Chem. Phys.* **35**, 1289.

Robinson, H., Dehmelt, H. G. & Gordy, W. (1954). *J. Chem. Phys.* **22**, 511.

Sternheimer, R. M. (1954). *Phys. Rev.* **95**, 736.

Toyama, M. (1959). *J. Phys. Soc. Japan*, **14**, 1727.

Van Bommel, A. J., Strijk, B. & Bijvoet, J. M. (1950). *Proc. Koninkl. Nederland Akad. Wetenschap*, **53**, 47.

Acta Cryst. (1963). **16**, 134

The Synthesis and Crystal Structures of some Alkaline Earth Titanium and Zirconium Sulfides

By Abraham Clearfield

National Lead Company, Titanium Alloy Division, Niagara Falls, New York, U.S.A.

(*Received* 26 *July* 1961 *and in revised form* 13 *April* 1962)

Barium titanium sulfide ($BaTiS_3$) and calcium, strontium and barium zirconium sulfides ($CaZrS_3$, $SrZrS_3$ and $BaZrS_3$) have been synthesized by the reaction of CS_2 with the respective ternary oxides at elevated temperatures. Barium titanium sulfide is hexagonal but its sulfur content decreases with increasing temperature of preparation. This results in a variation of unit cell dimensions from $a = 6{\cdot}752$, $c = 5{\cdot}810$ Å when prepared at 700 °C. to $a = 6{\cdot}77$, $c = 5{\cdot}74$ Å when prepared at 1100 °C. $BaTiS_3$ containing a stoichiometric or near stoichiometric equivalence of sulfur has the barium nickelate structure. As the sulfur content decreases the structure becomes increasingly disordered. $BaZrS_3$ is orthorhombic with $a = 7{\cdot}037$, $b = 9{\cdot}983$, $c = 7{\cdot}050$ Å and has a distorted perovskite structure. $SrZrS_3$ and $CaZrS_3$ have even more highly distorted perovskite structures and require orthorhombic unit cells with $a = 13{\cdot}49$, $b = 9{\cdot}79$, $c = 14{\cdot}23$ Å for $SrZrS_3$ and $a = 13{\cdot}07$, $b = 9{\cdot}58$, $c = 14{\cdot}05$ Å for $CaZrS_3$.

Introduction

Hahn & Mutschke (1956) prepared $SrTiS_3$, $BaTiS_3$ and $BaZrS_3$ by heating mixtures of the binary sulfides in sealed evacuated tubes for several weeks. The strontium and barium titanium sulfides were isomorphous and could be indexed by means of hexagonal, orthorhombic or tetragonal unit cells. These compounds were tentatively assigned the hexagonal $BaNiO_3$ structure (Lander, 1951). However, some serious discrepancies between the calculated and observed intensities were obtained. Barium zirconium sulfide was found to be dimorphic. The allotrope prepared below about 800 °C. was found to be tetragonal with $a = 4{\cdot}990$, $c = 5{\cdot}088$ Å and to have a perovskite structure. The high temperature form could not be indexed.

This paper describes the preparation of alkaline earth titanium and zirconium sulfides by the action of CS_2 on the corresponding ternary oxides together with additional observations on their structure.

Experimental

All of the titanates and zirconates used were c.p. grade (TAM Division, National Lead Company) and contained less than 0·2% total metallic impurities. Powder patterns of the ternary oxides showed the presence of only the desired phase. The sulfiding procedure was similar to that used for the preparation of ZrS_2 (Clearfield, 1958). Argon was bubbled through a tower containing CS_2 and the resultant gas mixture then led into a zircon combustion tube containing 10 g. of the ternary oxide in a carbon boat. The flow rate of the argon was fairly constant so that the amount of CS_2 entering the combustion tube was roughly proportional to the reaction time. Powder patterns were obtained with a G. E. XRD-3 X-ray unit and diffractometer using filtered Cu $K\alpha$ radiation. Aluminum powder and aluminum oxide were used as internal standards for the determination of accurate unit cell dimensions.

Barium titanium sulfide

The preparation of $BaTiS_3$ was carried out at one hundred degree intervals in the temperature range 400–1100 °C. Only small amounts (up to 30%) of sulfide were obtained in 4 hours time below 700 °C. However, the products obtained in 4 hours reaction